



UNIVERSITY OF LEEDS

This is a repository copy of *Studying bubble-particle interactions by zeta potential distribution analysis*.

White Rose Research Online URL for this paper:  
<http://eprints.whiterose.ac.uk/85195/>

Version: Accepted Version

---

**Article:**

Wu, C, Wang, L, Harbottle, D et al. (2 more authors) (2015) Studying bubble-particle interactions by zeta potential distribution analysis. *Journal of Colloid and Interface Science*, 449. 339 - 408. ISSN 0021-9797

<https://doi.org/10.1016/j.jcis.2015.01.040>

---

© 2015, Elsevier. Licensed under the Creative Commons Attribution-NonCommercial-NoDerivatives 4.0 International  
<http://creativecommons.org/licenses/by-nc-nd/4.0/>

**Reuse**

Unless indicated otherwise, fulltext items are protected by copyright with all rights reserved. The copyright exception in section 29 of the Copyright, Designs and Patents Act 1988 allows the making of a single copy solely for the purpose of non-commercial research or private study within the limits of fair dealing. The publisher or other rights-holder may allow further reproduction and re-use of this version - refer to the White Rose Research Online record for this item. Where records identify the publisher as the copyright holder, users can verify any specific terms of use on the publisher's website.

**Takedown**

If you consider content in White Rose Research Online to be in breach of UK law, please notify us by emailing [eprints@whiterose.ac.uk](mailto:eprints@whiterose.ac.uk) including the URL of the record and the reason for the withdrawal request.



[eprints@whiterose.ac.uk](mailto:eprints@whiterose.ac.uk)  
<https://eprints.whiterose.ac.uk/>

# Studying bubble-particle interactions by zeta potential distribution analysis

Chendi Wu, Louxiang Wang, David Harbottle, Jacob Masliyah and Zhenghe Xu\*

Department of Chemical and Materials Engineering, University of Alberta, Edmonton, Alberta  
Canada T6G 2V4

\*Corresponding Author: [zhenghe.xu@ualberta.ca](mailto:zhenghe.xu@ualberta.ca)

## Abstract

Over the last decade, Xu and Masliyah have pioneered an approach to characterize the interactions between particles in dynamic environments of multicomponent systems by measuring zeta potential distributions of individual components and their mixtures. Using a Zetaphoremeter, the measured zeta potential distributions of individual components and their mixtures were used to determine the conditions of preferential attachment in multicomponent particle suspensions. The technique has been applied to study the attachment of nano-sized silica and alumina particles to sub-micron size bubbles in solutions with and without the addition of surface active agents (SDS, DAH and DF250). The degree of attachment between gas bubbles and particles is shown to be a function of the interaction energy governed by the dispersion, electrostatic double layer and hydrophobic forces. Under certain chemical conditions, the attachment of nano-particles to sub-micron size bubbles is shown to be enhanced by in-situ gas nucleation induced by hydrodynamic cavitation for the weakly interacting systems, where mixing of the two individual components results in negligible attachment. Preferential interaction in complex tertiary particle systems demonstrated strong attachment between micron-sized alumina and gas bubbles, with little attachment between micron-sized alumina and silica, possibly due to instability of the aggregates in the shear flow environment.

**Keywords:** zeta potential distribution; multicomponent dispersions; particle interactions, nano particle-bubble attachment.

## Introduction

Colloid is a term often used to describe a dispersion of particles in a liquid, with at least one characteristic length scale between 5 nm and 100  $\mu\text{m}$ . [1] Particles in this communication are broadly referred to as discrete and dispersed solids and gases. Discrete particles of nanometer length scales exhibit little inertial contribution to the macroscopic mobility which is often governed by thermal diffusion ( $kT/a$ ), the Brownian motion of particles, where  $k$ ,  $T$ , and  $a$  are Boltzmann constant, absolute temperature, and particle size, respectively. In nanotechnology, colloidal particles opened up new avenues of research that has led to the development of numerous high tech and commercial products. Such products are used widely in everyday life such as nano medicines, health care and personal protection products, paints and foods, energy conversion and production, water purification and environmental protection, etc. Colloids are extremely abundant in process engineering, particularly in mineral processing where the depletion of easy processing minerals to meet the ever-growing demand of an expanding global population has led to the exploration of low grade mineral deposits that require fine grinding to liberate the valuables from the gangue. Traditional processing techniques that were designed to separate and process coarser particles are now becoming inadequate or inefficient to process the more challenging colloidal particles.

When dispersed in aqueous environment colloidal particles have a tendency to interact with neighboring particles in close proximity to form aggregates or clusters by attraction or remain dispersed by repulsion. The balance between attraction and repulsion depends on the surface charge characteristics that are governed by material type and solution chemistry. When submerged in an aqueous environment, particles can attain a surface charge through a number of mechanisms. For example, metal oxide particles undergo hydrolysis followed by ionization (dissociation) of the surface metal hydroxyl groups, leaving behind an often negatively charged surface. Inherent isomorphic substitution of higher valence cations by lower valence cations in silicon dioxide tetrahedral and aluminum oxy-hydroxyl octahedral sheets of layered clays (kaolinite and illite) results in a permanent positive charge deficiency and hence negatively charged basal planes.

Theoretically, the total interaction potential between colloidal particles can be described by the DLVO (Deryaguin, Landau, Verwey and Overbeek) theory.[2, 3] However, the interaction behavior as theoretically described by DLVO is somewhat limited when considering a wide variety of interaction phenomena at short-range. Non-DLVO forces that are understood to a lesser extent can become dominant, shielding the predicted DLVO-type behavior. Such non-DLVO forces include repulsive hydration force for hydrophilic surfaces,[4-8] attractive hydrophobic force for hydrophobic surfaces,[9-11], repulsive steric force between polymer brush-bearing surfaces,[12, 13] attractive bridging force,[14] attractive depletion force,[15] short-range protrusion and long-range undulation forces.[16] Although these non-DLVO forces have been studied extensively, the underlying theory is often limited to approximations determined through empirical fitting parameters. Of the non-DLVO forces, hydrophobic forces are considered the only driving force for recovery of fine minerals by flotation. Whilst studied extensively for over 30 years, the exact nature of the hydrophobic force remains an area of intense debate.[17]

### **Measurement of colloidal and surface forces**

Although the elegant description of the classical DLVO theory has been realized for several decades, a more advanced understanding of colloidal and surface forces has progressed rapidly with the introduction of sophisticated force measurement devices such as: surface forces apparatus (SFA), atomic force microscopy (AFM) and thin film balance (TFB). Such devices have the capability to measure forces in the pN – nN range, with distance resolution below 1 nm.

A similarity of all three methods is that the force – distance profiles are frequently measured at low approach velocity to minimize hydrodynamic effects, although recently there has been emphasis on studying hydrodynamic effects between a solid particle and a bubble,[18, 19] a solid particle and a deformable droplet,[20, 21] and two oil droplets[22, 23] using high speed AFM. Whilst those fundamental forces govern bubble–particle attachment and detachment, there is an additional sub-process in flotation, namely collision that is strongly dependent on hydrodynamic conditions. Recently, an integrated thin film drainage apparatus (ITFDA) has been developed by Xu and Masliyah to consider the hydrodynamic phenomena. Producing a millimeter size gas bubble at the tip of a glass capillary attached to a speaker diaphragm, the approach velocity of a

gas bubble towards a target surface can be accurately controlled within the range from  $\mu\text{m/s}$  to  $\text{mm/s}$ , providing an opportunity to study hydrodynamic resistance on the drainage kinetics of thin liquid films. Coupled with separation distance, the interaction force between two surfaces can be accurately measured by a bimorph force sensor to which the lower surface is intimately attached. Investigating the role of bubble approach velocity and surface hydrophobicity between a gas bubble and a glass sphere, the ITFDA experiments showed that the normalized force barrier (film drainage resistance) increased linearly with approach velocity, which can be lessened by increasing the hydrophobicity of the target surface (i.e. the normalized force barrier at an equivalent approach velocity decreases with increasing hydrophobicity of solid surfaces).[24, 25] For a strongly hydrophobic surface under a critical flow condition (approach velocity  $\sim 0.24 \text{ mm/s}$ ) the contributions from dispersion forces and hydrodynamic resistance are completely diminished by the strong and long-range hydrophobic force.

Measurements in an environment that are more representative of a dynamic process provide an opportunity to form a more complete understanding of the surface or colloidal forces. For example, most surface forces technique operate under the conditions where hydrodynamic effects are negligible, and the surface studied is often a small fraction of the total surface area. The results obtained with these techniques are extremely informative. However, when considering the interactions in dynamic environments (sheared systems) between real particles of varying surface characteristics in i) surface roughness, ii) surface contamination and iii) mixed mineralogy (target mineral and gangue), the overall behavior is considerably more challenging to determine, with the classical theory and extended DLVO theory possibly resulting in an under or over estimate of the interaction behavior.

### **Measuring interaction potential by electrophoretic mobility (zeta potential)**

Over the last decade Xu and Masliyah have recognized that different particles could possess different surface properties and have successfully pioneered an approach to characterize the interaction potential between real particles in dynamic environments. Using a Zetaphoremeter (CAD Instrumentation, Z3110), the electrophoretic mobility or zeta potential distributions of individual and mixed (binary) systems can be measured to identify the attachment conditions between two components. The technique has been applied to study many different colloidal or

multicomponent systems, including bitumen liberation and flotation (slime coating) in oil sands processing,[26] deinking in paper recycling,[27] uptake of copper and collector by sphalerite in gypsum saturated solutions (minerals flotation),[28, 29] and heterocoagulation in formulation of chemical-mechanical polishing (CMP) slurries.[30] A brief summary of the systems considered and the main findings are provided in Table 1.

Table 1. Particle interactions in complex binary mixtures studied by zeta potential distribution analysis.

<b>Authors</b>	<b>System(s) studied/ application</b>	<b>Conclusions</b>
Liu et al.[26, 31]	Bitumen – kaolinite and Bitumen – montmorillonite (Oil sands processing)	<p>1] Strong slime coating of bitumen by montmorillonite in the presence of calcium ions, with no slime coating by kaolinite.</p> <p>2] Slime coating potential confirmed by long range colloidal force measurement (AFM – microscale colloidal force measurement). Force profiles reasonably fitted by the classical DLVO theory.</p> <p>3] Slime coating potential by montmorillonite and not kaolinite reconciled by the strong adhesion force between montmorillonite and bitumen but not between kaolinite and bitumen in the presence of calcium ions.</p> <p>4] High specific surface area, cationic exchange capacity and the consequent high charge density (<math>Ca^{2+}</math>) of montmorillonite accounted for the strong bridge of bitumen and fines by calcium ions.</p>
Liu et al.[32] Zhao et al. [33]	Bitumen – silica (Oil sands processing)	<p>1] Strong attraction leading to heterocoagulation of bitumen and silica measured in 1 mM KCl at pH 10.5 with 1 mM calcium addition. The strong adhesion and long range attraction as verified by AFM contribute to poor bitumen liberation from sand grains.</p>
Liu et al.[34, 35]	Bitumen – fines from tailings (good and poor processing ore) And extracted bitumen froth (Oil sands processing)	<p>1] No slime coating observed for bitumen mixed with fines extracted from a good processing ore in KCl + <math>Ca^{2+}</math> aqueous solution and process water, in contrast to severe slime coating of bitumen in the same water chemistries for solids extracted from poor processing ores.</p> <p>2] Good agreement of the results with the slime coating properties of the dispersed bitumen froth from both the good and poor processing ores.</p>

		3] Zeta potential distribution measurements confirmed by colloidal force measurement.
Ding et al. [36]	Bitumen – illite (Oil sands processing)	1] Detrimental effect of illite slime coating on bitumen flotation performance observed in acidic conditions. 2] Slime coating of bitumen by illite mitigated by adjusting pH of the tailings water to 8.5.
Liu et al.[27]	Talc – ink particles (Paper recycling)	1] Effective flotation of fine ink particles by carrier talc particles as a result of heterocoagulation between talc and ink particles in the presence of calcium chloride and sodium oleate. 2] Deposition of treated talc with a propriety cationic chemical on ink particles at pH 4, 6 and 9 in the absence of any further chemical additives.
Lin et al.[30]	Silica – ceria nanoparticles (Chemical Mechanical Polishing slurries)	1] Gradual deposition of positively charged ceria particles (~5.4 nm) on negatively charged silica particles (~132.2 nm). 2] Shift of distribution peak from -24 mV to 28mV with increasing ceria:silica particle ratio from 1:20 to 2:5. 3] The least stable particle suspension measured at a ceria:silica particle ratio of 1:10 with the corresponding frequency peak at 14 mV.
Deng et al. [29]	Silica and sphalerite particles in gypsum supersaturated solutions (Minerals flotation)	1] Significant reduction in the magnitude of the silica and sphalerite zeta potential when dispersed in gypsum supersaturated solutions due to the adsorption of calcium ions, leading to poor recovery and selectivity of sphalerite flotation in real flotation systems.
Deng et al. [28]	Sphalerite – sodium isopropyl xanthate (SIPX) (Minerals flotation)	1] Activation of sphalerite by copper (specific adsorption or ion exchange of zinc ions) and subsequent uptake of SIPX demonstrated by zeta potential distribution measurements. 2] Copper and SIPX adsorption on sphalerite substantially suppressed in the presence of 800 ppm calcium and gypsum saturated solutions, a result of charge neutralization by calcium ion adsorption.
Forbes et al. [37]	Kaolinite – chalcopyrite	1] Slime coating potential of chalcopyrite particles by kaolinite particles proved inconclusive due to significant overlap of the zeta potential distributions of the individual components.

When zeta potential distributions of two different particle (solid, liquid, gas) species (A and B, see Fig. 1a) are distinguishable, the level of interaction between these two types of particles in a binary mixture can be qualitatively assessed from the resulting zeta potential distribution as described below. If particles A and B do not attract each other, a bimodal zeta potential distribution of the mixture with two peaks being centered on the locations of two individual (single) species distributions ( $\zeta_A, \zeta_B$ ) as shown in Fig. 1b is observed. With the hydrodynamic interactions of moving particles at different electrophoretic mobilities, a slight shift of the two distribution peaks towards one another may be observed, commonly known as electrophoretic retardation. If particles A and B are strongly attractive, the two individual distributions will transform into a single modal distribution of the binary system. The location of the single distribution peak will be either at  $\zeta_A$  or  $\zeta_B$ , depending on whether particles A completely cover particles B or vice versa. For the example shown in Fig. 1c, particles B completely cover particles A, screening the zeta potential contribution of particles A. In this case, an excess number of individual components B as indicated in the inset of Fig. 1c may exist. Depending on the ratios of the two particle species, strong interaction can also be inferred from a single modal zeta potential distribution of the binary mixture as shown in Fig. 1d, with the peak being located at  $\zeta_{A/B}$  which is intermediate to the two peak positions of  $\zeta_A$  and  $\zeta_B$ , corresponding to zeta potential distribution peaks of individual components. Such zeta potential distribution characteristics of a binary system indicate incomplete coverage of particles A by particles B or vice versa, mainly due to insufficient particles available to fully cover the other type of particles. For weaker particle attractions, two or three peaks in zeta potential distributions of binary mixtures are likely to be observed. Fig. 1e shows a tri-modal distribution accounting for the partial coverage of particles A by particles B ( $\zeta_{A/B}$ ) and two other distribution peaks that correspond to  $\zeta_A$  and  $\zeta_B$  of remaining individual particles A and B as a result of weak attraction and hence less efficient attachment. For weak attractions, the number and position of the peaks depend on both the strength of the attraction and the number ratio of the two interacting species.

While reference is made to strong and weak interactions, those interactions as described by zeta potential distributions remain highly qualitative. However, previous research has shown excellent agreement between zeta potential distributions of binary mixtures and interaction forces as measured by AFM.[33] Due to its versatility to determine particle interactions of

complex multicomponent systems where highly sophisticated surface forces apparatus and atomic force microscope cannot be used, the zeta potential distribution measurement was used in the current study to determine attachment characteristics between sub-micron size gas bubbles and solid (silica and alumina) particles. The degree of attachment was controlled by varying the electrostatic and hydrophobic forces. The critical role of gas nucleation by hydrodynamic cavitation on solid particles in bubble-particle attachment is also illustrated. The research demonstrates the simplicity of the technique to provide an understanding of preferential particle attachment in complex multicomponent systems.

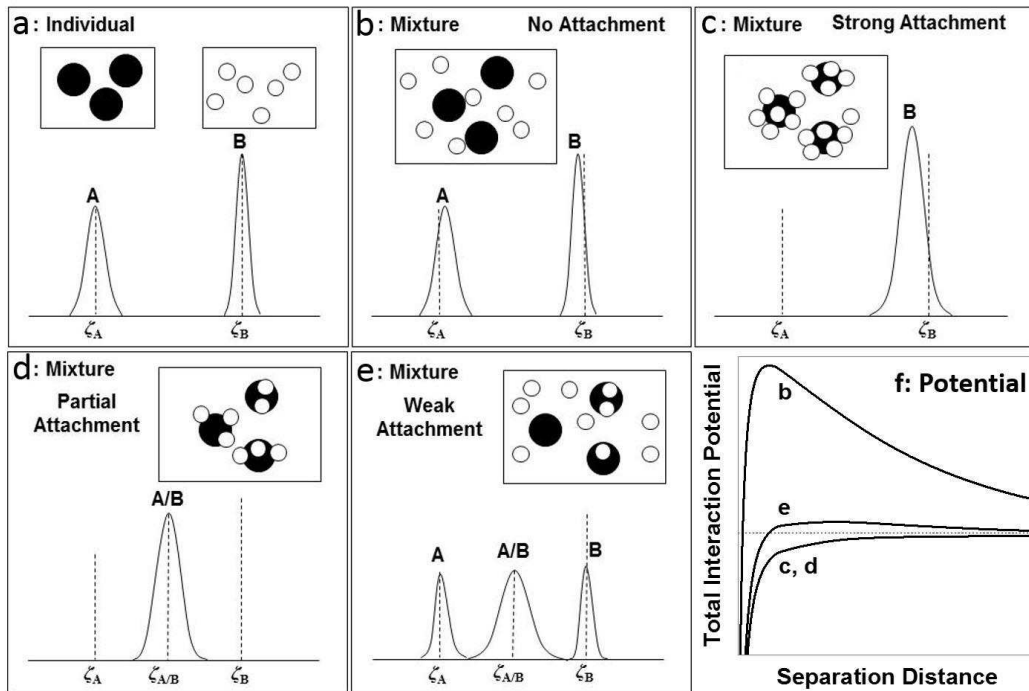


Figure 1. Possible outcomes for particle attachment in a binary mixture as determined from the zeta potential distribution analysis. a: distributions of two individual components overlaid; b: distribution of binary mixture without attraction between the two components; c: distribution of binary mixture with strong attraction and component B covering component A; d: distribution of binary mixture with strong attraction between the two components, but insufficient components A to cover B or vice versa; e: distribution of binary mixture with weak attraction where both individual components and aggregates exist; f: schematic representation of the total interaction potential (DLVO theory[2, 3]) between components A and B for systems b, c/d and e, respectively.

## Materials and Methods

Milli-Q water with a resistivity of 18.2 M $\Omega$  was used in the preparation of all solutions and suspensions. The aqueous solutions were further filtered (0.1 $\mu$ m, Millipore) prior to their use to avoid potential contamination of fine particles. Reagent grade KCl (Fisher Scientific, Canada) was used as the background electrolyte and reagent grade HCl (Fisher Scientific) and NaOH (Sigma-Aldrich, Canada) were used to adjust pH. Surfactants and frothers such as: sodium dodecyl sulphate (SDS, Sigma-Aldrich), dodecylamine hydrochloride (DAH, Acros Organics, Canada) and DF250 (Dow Chemical Canada, Inc) were used to i) promote generation and stabilization of sub-micron size gas bubbles, and ii) adjust surface potential of the generated gas bubbles and fine particles in suspension. Two types of solids, Al<sub>2</sub>O<sub>3</sub> and SiO<sub>2</sub> were studied. Nano size alumina and silica particles ( $d_{50} \sim 15$  nm, provided by the manufacturer) were supplied by MKnano (Canada), while micron size alumina particles ( $d_{50} = 868 \pm 115$  nm) were purchased from Fisher Scientific (Canada), and silica particles ( $d_{50} = 939 \pm 162$  nm) supplied by U.S. Silica (USA).

Preparation of particle suspensions: All suspensions were prepared by adding a tea spoon of solids to 60 mL aqueous solutions (Milli-Q water plus desired chemical loading) and sonicated for 15 min to disperse the aggregated particles. After sonication the suspension was allowed to settle for 10 minutes. Several drops of the supernatant were then taken and gradually added to 50 mL aqueous solutions of the same water chemistry as solid suspensions. The diluted suspension was injected into the measurement cell of Zetaphometer with a syringe. The number of particles in the suspension is tracked by the instrument using the count function associated with each zeta potential measurement. The concentration of the particles in the suspension was adjusted by dilution (to minimize the electrophoretic retardation effect) until the number of particles reaches 20 to 100 that could be effectively identified and tracked by the Zetaphometer. The number of sub-micron size bubbles in its dispersion of the same water chemistry as particle suspensions is adjusted in the same manner. Mixing particle suspension and bubble dispersion at 1:1 volume ratio would lead to a binary mixture of the same number of solid particles and bubbles for zeta potential distribution measurement.

Preparation of bubble suspensions: A high speed agitator (Model 100DLC, Ross, Canada) was used to generate gas bubbles by hydrodynamic cavitation in a custom-designed, vertically baffled cylindrical high intensity agitation (BHIA) cell. All the aqueous solutions were prepared by dissolving the desired chemicals in Milli-Q water at room temperature. To enhance the generation of sub-micron size bubbles, aqueous solutions were first pre-saturated with tanked air (Praxair) at 8 °C for 24 hr, with saturation at lower temperature being intended to dissolve as much air as possible for bubble generation. Sub-micron size gas bubbles were generated by hydrodynamic cavitation in the BHIA cell at a fixed agitation speed of 2200 rpm and agitation time of 40 min. The sub-micron size gas bubbles generated using this method have a bubble size of  $d_{50} \sim 350$  nm which remain stable for up to 24 hr with the presence of surfactant.[38]

A Rushton impeller 5.7 cm in diameter and 1.2 cm in blade width was used throughout the study. Entrainment of ambient gas was minimized by operating the cell at maximum volume (350 mL) such that the cell lid remained in contact with the liquid. The cell lid was secured with two thumbscrews and a gastight seal achieved by several gaskets, ensuring that the seal was airtight. As shown in Fig. 2, the BHIA cell included two sampling ports, one at the top and the second near the bottom of the cell, which were used to connect the BHIA cell to the Zetaphoremeter, enabling the transfer of the prepared dispersions for zeta potential distribution measurement. Prior to fluid transfer, the bubble dispersion was gently stirred in the BHIA cell for 30 min, allowing the dispersion to cool after vigorous mixing and the adjustment of dispersion pH if required.

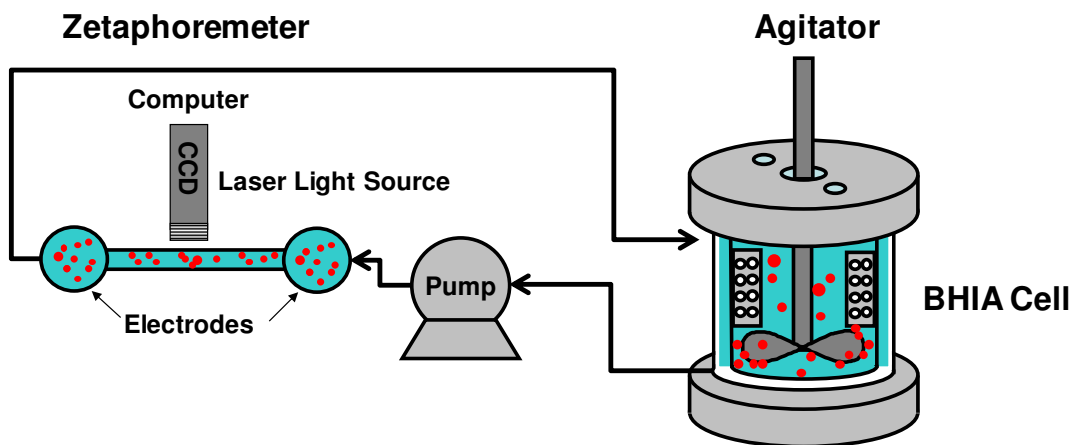


Figure 2. Schematic diagram of the experimental setup linking the BHIA cell with a high speed agitator to the Zetaphoremeter via a peristaltic pump.

Zeta potential measurement: Bubble – solid interactions were measured using a commercial Zetaphoremeter (CAD Instrumentation, Z3110) by analysis of zeta potential distributions.[26] Desired dispersions and/or suspensions were pumped from the BHIA cell (or glass beaker, see Protocol I below) into the measurement cell which is a rectangular quartz micro-electrophoresis cell with a pair of palladium-coated electrodes being incorporated. After pumping the test sample into the measurement cell, the two valves at either end of the measurement cell were closed to prevent any unnecessary fluid disturbances that may interfere with accurate measurement of electrophoretic mobility. Passing an electric field through the aqueous phase, the mobility of the dispersed phase on a thin horizontal layer was monitored by a CCD camera, with the mobility of 20 – 100 particles/bubbles being tracked and analyzed to determine their zeta potentials by the Smoluchowski approximation. Each sample was measured at least five times, each time replacing the dispersion or suspension in the measurement cell with fresh sample. The zeta potential values of five repeat measurements (100-500 values) were used to plot the zeta potential distribution histogram reported throughout the study.

To study particle – gas bubble interactions, two protocols of mixing were considered. In Protocol I, the solid dispersion prepared using the previously described procedure was mixed in a glass beaker with an equal volume of sub-micron bubble dispersion generated in the BHIA cell. The newly prepared sample was mixed in the beaker for 30 min using a magnetic stir bar, and the pH of the mixture was adjusted if required. In Protocol II, solid particles were added to the air saturated aqueous phase prior to bubble generation. The mass of particles added to the aqueous solution was determined to achieve the balance in the number of particles and gas bubbles at approximately 1:1. High intensity agitation was applied to fine particle suspensions, where gas bubbles may nucleate in-situ on solid surfaces. The second protocol, a method highly desirable for fine particle flotation,[39, 40] allows us to study relative efficiency of bubble-particle attachment by gas nucleation as compared to the case by bubble-particle collision as in the case of Protocol I.

## **Results and Discussion**

### **Individual components**

The method for studying particle – particle interaction by zeta potential distribution measurement relies on two components having distinctly different zeta potential distributions under the same chemical conditions. To optimize the conditions for further study, the average zeta potentials for the three components of interest (silica, alumina and gas bubble) were first measured. In this study, solid particles of two different particle size ranges from nano meter to micron meter were used. The background electrolyte was 1 mM KCl and the solution pH adjusted either acidic or basic from the natural pH. The results are given in Fig. 3. Over the pH range from 2.5 to 10.5, the alumina particles showed a clear isoelectric point (iep) of pH ~9.4, in good agreement with the data reported previously.[41] For the silica particles, the zeta potential remained negative across the pH range studied with the iep at a pH < 2.5. Similar to the silica particles, the gas bubbles generated in the BHIA cell carried a negative surface potential, with the magnitude of the zeta potential being approximately the same as the zeta potential of silica particles in the pH range from 4.5 to 10.5.

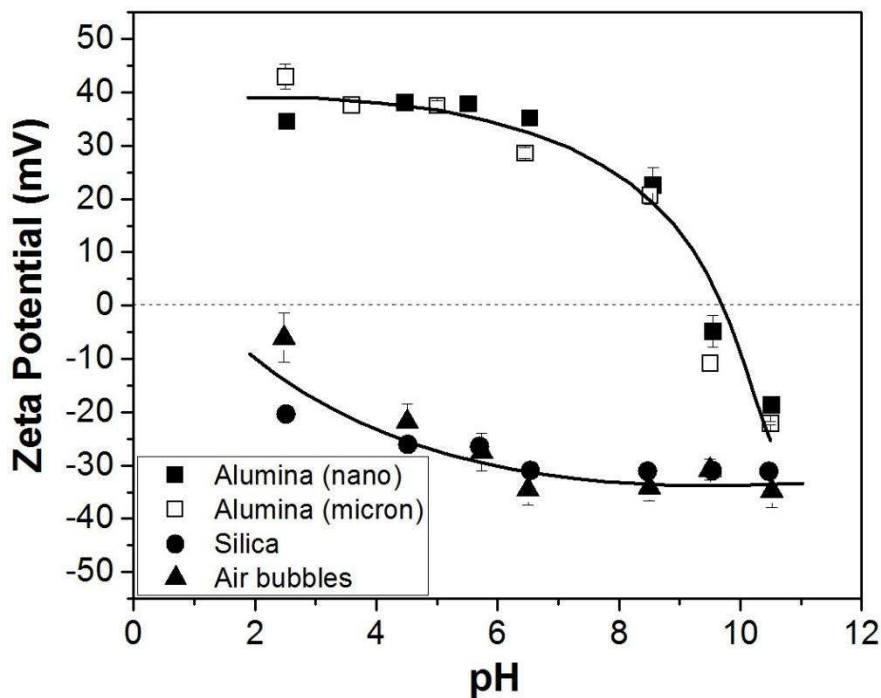


Figure 3. Zeta potential of alumina and silica particles, and gas bubbles as a function of solution pH. Background electrolyte: 1 mM KCl. The error bars represent the standard deviation of five repeat measurements.

Comparing all four zeta potential curves, it is evident that the alumina samples provide a substantial contrast to the silica and gas bubbles over a wide pH range. Such a drastic contrast provides an opportunity to study the interaction potentials between alumina particles and gas bubbles or silica particles. However, the similar zeta potentials measured under the current condition for silica and gas bubbles indicate that the interaction between them could not be determined with the current method.

For the above-mentioned reason, zeta potential distribution measurements were first completed using micron-sized alumina particles and gas bubbles at their natural pHs (mixed system pH ~5.3) in 1 mM KCl. The zeta potential distribution of individual components was measured first as baseline, followed by the measurement of the binary mixture. For the individual components, the results in Fig. 4 show single modal distributions for both samples, with the peaks being located at 39 mV and -30 mV for the alumina particles and gas bubbles, respectively. When the two were mixed together at an equal volume ratio, a single distribution was measured, with the peak being located at -12 mV. This characteristic of two individual component distributions merging to form a single distribution with the peak being positioned closer to the distribution peak of gas bubbles indicates a strong attachment of gas bubbles to alumina particles. Such a strong attachment is expected when considering a strong attractive force between particles of opposite zeta potentials. The observed configuration of gas bubble attaching to alumina particle is not unexpected when considering that the alumina particles ( $d_{50} \sim 868$  nm) are of diameters twice greater than the diameter of the gas bubbles ( $d_{50} \sim 350$  nm).[38] Furthermore, the alumina particles are not fully covered by the gas bubbles due to insufficient number of bubbles present in the system of almost equal number of gas bubbles and solid particles as controlled on purpose for the experiments.

### **Surfactant and frother solutions**

Chemical additives in the form of collectors and frothers are widely used in flotation. These chemical additives intentionally or inevitably modify surface properties of bubbles and/or solids for the enhanced attachment. In this section, the effect of collector and/or frother addition on bubble-particle attachment is studied.

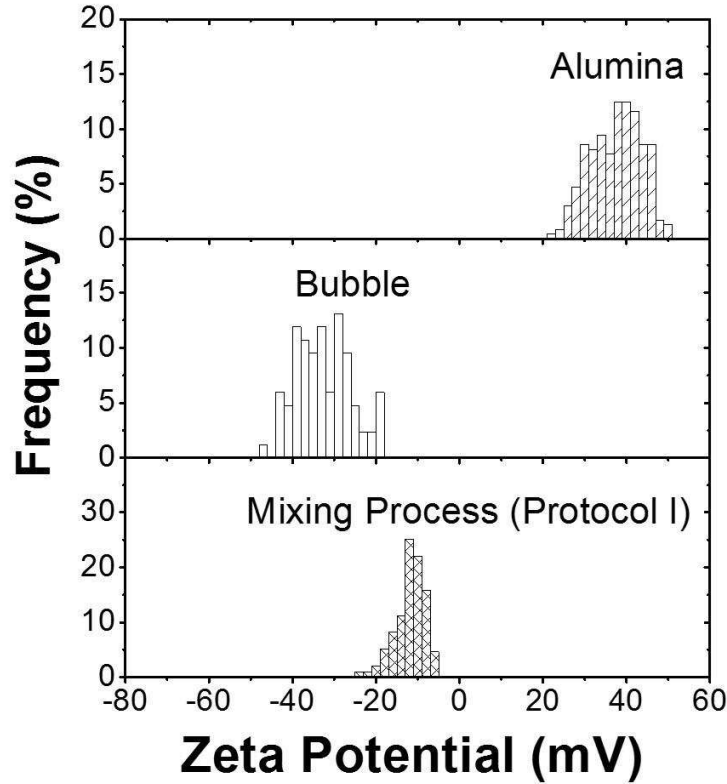


Figure 4. Zeta potential distribution of gas bubbles and micron-size alumina particles in 1 mM KCl solution at pH = 5.3, measured as individual components and a binary mixture.

SDS solutions: Sodium dodecyl sulphate (SDS),  $\text{CH}_3(\text{CH}_2)_{11}\text{OSO}_3\text{Na}$  is an anionic surfactant widely used as detergent and collectors in oxide flotation. With a 12 hydrocarbon tail attached to a hydrophilic sulphate head group, SDS has a critical micelle concentration of 8 mM at 25 °C. As shown in our previous study,[38] SDS readily adsorbs at the bubble-water interface, reducing the bubble zeta potential, i.e., becoming more negative. For example at pH 6 (Fig. 5), the zeta potential distribution peak of the bubbles in the presence of SDS shifted from -38 mV to -48 mV, confirming the partition of the ionized SDS molecules at the bubble-water interface. The zeta potential of the alumina particles in the presence of SDS at pH 6 remains positive with the peak value of 37 mV being similar to the case of no SDS addition. Although the anionic SDS molecules are anticipated to adsorb on positively charged alumina surface to reduce the zeta potential of alumina particles, the limited adsorption of SDS molecules at its low concentration of 0.01 mM as compared to its critical micelle concentration of 8 mM appears to be insufficient to cause a noticeable change in zeta potential of alumina. Similar results were reported

previously.[42, 43] Measuring the zeta potential distribution of the binary mixture using Protocol I (mixing process) and Protocol II (in-situ gas nucleation) leads to a single modal zeta potential distribution with the peak being located around -12 mV in both cases. With a strong attractive electrical double layer force, the attachment of one component to the other is confirmed. In this case, the attachment is not affected by the Protocol whether the bubble was nucleated in-situ on solid surface or bubbles generated were attached to the solid surface upon collision. In both cases, nano size alumina particles deposited on the larger size bubbles with only partial coverage achieved, as indicated by the location of the binary mixture distribution relative to the two individual distributions.

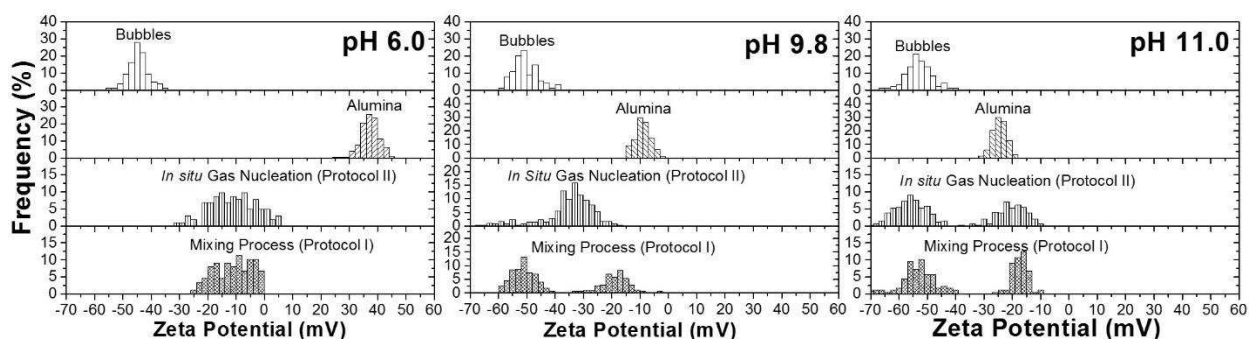


Figure 5. Zeta potential distribution of nano size alumina particle suspensions and gas bubble dispersions individually or as a mixture in 0.01 mM SDS + 1 mM KCl solution at pH 6.0, 9.8 and 11.0.

It is interesting to note that in the presence of SDS increasing dispersion pH to 9.8 did not further decrease zeta potential of bubbles. Considering the fully ionized nature of SDS at both pH 6.0 and 9.8, it is not surprising to see the absence of zeta potential change with increasing pH. At pH 9.8, the zeta potential of alumina particles remained around -10 mV with the addition of 0.01 mM SDS, indicating very limited adsorption of SDS on the particle surface. For the binary systems, the mixtures prepared using Protocol I (Bottom) led to two distinct distribution peaks at around -17 mV and -51 mV, respectively. These two zeta potential distribution peak values were in close agreement with the zeta potential distribution peak values of two individual components prior to mixing (Top), indicating the absence of attraction between alumina particles and gas bubbles. Although limited adsorption of SDS on alumina particles would make them hydrophobic, the electrostatic repulsion between negatively charged gas bubbles and alumina particles prevented the bubbles attaching to the particles. In contrast, very different zeta potential

distribution was observed when the binary system was prepared using Protocol II. In this case, only a single modal zeta potential distribution was obtained with the peak position of -31mV located in-between the peak positions of individual components of alumina particles (-10 mV) and gas bubbles (-55 mV), indicating the formation of gas bubble-alumina particle aggregates. This is an important finding as it illustrates the heterogeneous gas nucleation on weakly hydrophobic alumina particle surfaces to achieve particle aeration, despite the presence of electrostatic repulsive forces that prevented bubble-particle attachment. It is also plausible that the nano size bubbles generated by homogeneous nucleation in bulk liquid subsequently attached to alumina particles by high intensity agitation providing sufficient kinetic energy of bubbles and particles to overcome the energy barriers dominating the interaction potential as observed by Protocol I. Unfortunately the current study was not able to discern this latter attachment mechanism. Nevertheless, the observed attachment of gas bubbles to alumina particles in a system prepared by Protocol II support the concept of enhancing fine particle flotation by hydrodynamic cavitation. Hydrodynamic cavitation was thought to promote the formation of gas envelopes (hemi-spheres or caps) on hydrophobic solid particles that remain attached under the high intensity agitation.[44] Such hydrodynamic cavitation results in the successful ‘frosting’ of the particle surface,[45] further enhancing local hydrophobicity of the solid, which leads to a two-stage aeration process that includes heterogeneous nucleation followed by attachment to flotation size bubbles.[45]

In the presence of SDS at pH 11, the zeta potential distribution of the gas bubbles remained the same as at pH 6.0 and 9.8, while the zeta potential distribution of alumina particles shifted slightly to more negative values of -25 mV. Under this condition a strong electrostatic repulsive interaction potential between gas bubbles and alumina particles is anticipated. As a result, Fig. 5 shows no bubble-particle attachment observed regardless of whether the binary mixture was prepared using Protocol I or Protocol II. It is therefore reasonable to state that in order to realize two-stage bubble aeration mechanism to enhance fine particles flotation, it is important to fine tune bubble-particle interaction potentials so that heterogeneous gas nucleation by hydrodynamic cavitation is favored.

DAH solutions: Dodecyl amine hydrochloric acid (DAH),  $\text{CH}_3(\text{CH}_2)_{11}\text{NH}_2\text{HCl}$  is a cationic surfactant with a critical micelle concentration of 13 mM. The amphiphilic nature of the DAH molecules results in their partitioning at the air-water interface, modifying the zeta potential and the hydrophobicity of the gas bubble. In the case of gas bubble – alumina particle, the zeta potential distribution technique becomes unsuitable to study bubble-particle interaction potentials due to significant overlap of the zeta potential distributions with the peak being measured at 29 mV and 23 mV for the gas bubbles and alumina particles, respectively (data not shown). The positive zeta potential measured for the gas bubble confirms substantial adsorption of the collector at the air-water interface. Based on this limitation, focus was given to studying the interactions between DAH stabilized gas bubbles and negatively charged silica particles with the results given in Fig. 6.

In 1 mM KCl solution at pH 6.5, the zeta potential of silica remained close to -25 mV with the addition of 1 mM DAH. Similar to the little change of alumina zeta potential with the presence of 0.01 mM SDS, a negligible change of silica zeta potential is probably also due to the low concentration of DAH. In contrast, a significant increase in zeta potential of bubbles from -25 mV to 47 mV was observed as a result of DAH adsorption. Upon mixing (Protocol I), a single zeta potential distribution is measured, with the zeta potential distribution peak located at -17 mV, showing a strong attractive force between the two components of opposing charge that is sufficient to deposit nano size silica (~15 nm) onto sub-micron size bubbles (~350 nm), indicated by the single distribution situated closer to the zeta potential distribution peak of silica particles.

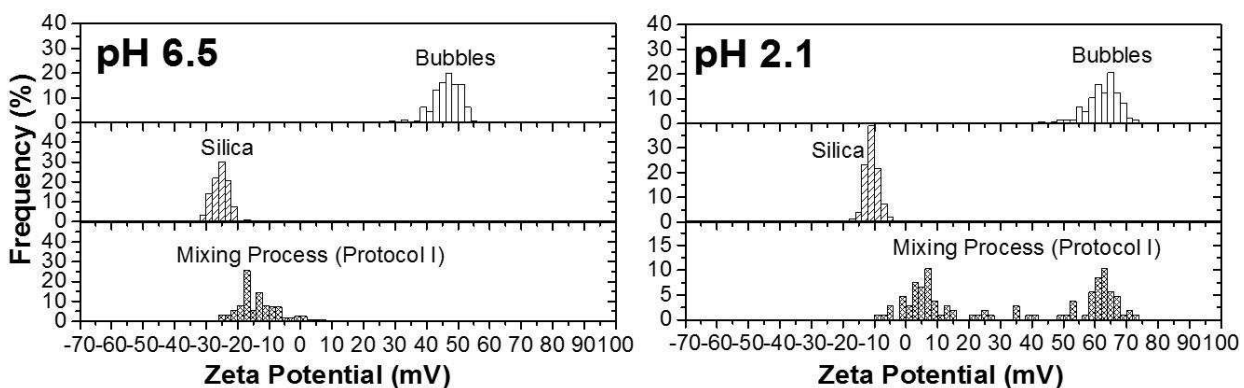


Figure 6. Zeta potential distribution of nano size silica particles and gas bubbles prepared in 1 mM DAH + 1 mM KCl solution at pH 6.5 and 2.1.

At pH 2.1, the addition of DAH had a negligible effect on zeta potential of silica particles, with the zeta potential distribution peak at -12 mV. At this pH, silica particles carry a negligible surface charge, leading to a negligible adsorption of DAH on silica particles.[46] As a result, the silica particles remain highly hydrophilic. When mixing the two components together by Protocol I, two distinct distributions were measured, with the peaks being located at zeta potential values corresponding to the peaks of the individual components. Applying the Hogg-Healey-Fuerstenau (HHF) approximation,[2] one would anticipate a weak attractive electrical double layer force. The absence of bubble-particle attachment suggests an overall repulsive interaction due to the repulsive van der Waals forces with strong short range repulsive hydration force as a result of highly hydrophilic nature of silica surfaces. Since the electrostatic attraction between silica particles and gas bubbles in the presence of 1 mM DAH at pH 6.5 and pH 2.1 would be very similar, the observed strong attachment of silica particles to gas bubbles at pH 6.5, but not at pH 2.1 suggests the critical role of hydrophobic forces in bubble-particle attachment at pH 6.5, i.e., the adsorption of DAH on silica surface at pH 6.5 changed the hydrophobicity of silica, whilst the silica surface at pH 2.1 remained hydrophilic due to deficiency of DAH adsorption.

DF250 solutions: To further isolate the electrostatic and hydrophobic force contributions, a polypropylene glycol methyl ether,  $\text{CH}_3\text{-(O-C}_3\text{H}_6\text{)}_x\text{-OH}$  known as Dowfroth 250 (DF250), is considered. DF250 is a non-ionic surfactant and is anticipated to adsorb at the air-water interface which will reduce the hydrophobicity of bubbles without significant impact on bubble surface charge. Since DF250 is a neutral molecule, its effect on alumina and silica particles would be minimal. As such, the predominant long range interactions force was expected to be limited to the electrical double layer force and van der Waals forces. Due to similar zeta potential values of the silica particles and gas bubbles (see Fig. 9), only the interactions between gas bubbles and alumina particles were considered.

Figure 7 shows the zeta potential distributions of the individual species and binary system in the presence of 0.1 mM DF250 as a function of pH. The binary mixture system was prepared using Protocol I. In 1 mM KCl + 0.1 mM DF250 solution at pH 6.5, the zeta potential

distribution peaks of the gas bubbles and alumina particles were located at -37 mV and 33 mV, respectively. The observed zeta potential distribution peak value of gas bubbles is slightly more negative in the presence than in the absence of 0.1 mM DF250, indicating adsorption of DF250 molecules at bubble-water interface. For alumina particles, the zeta potential distributions are almost identical in the presence and absence of 0.1 mM DF250, suggesting a negligible adsorption of DF250 on alumina particles. Upon mixing of the two components, a single modal zeta potential distribution was measured with the peak being located at -16 mV, indicating a strong attachment of alumina particles to gas bubbles. Despite the hydrophilic nature of alumina in such solutions, such a strong attachment is anticipated from strong electrostatic attraction due to the opposite surface charges of alumina particles and gas bubbles in 1 mM KCl + 0.1 mM DF250 solution of pH 6.5. Due to hydrophilic nature of alumina particles, the particles and bubbles are most likely attracted to each other at the deep primary minimum of interaction potential without the formation of three phase contact line. Such an attachment mode was illustrated in literature,[47] which supports the concept of contactless flotation of fine particles, controlled mainly by electrostatic attraction.[48]

At higher pH, the presence of 0.1 mM DF250 showed a negligible effect on zeta potential distributions of alumina. For example, the zeta potential distribution peak of alumina at 9 mV and -22 mV for pH 8.5 and 11 in the presence of 0.1 mM DF250 is almost the same as in the case without DF250. These results support the hypothesis that neutral DF250 molecules do not adsorb on alumina particles. For bubbles, the zeta potential distribution peak at -48 mV and -58 mV for pH 8.5 and 11 is slightly more negative than the zeta potential distribution peak values of -30 mV for the gas bubbles at these two pHs without DF250. The more negative zeta potential value of gas bubbles with 0.1 mM DF250 addition further confirms adsorption of DF250 molecules at the air-water interface even at these high pHs.

It is interesting to note a bimodal zeta potential distribution of mixtures at pH 8.5. In this case, the zeta potential distribution peak corresponding to alumina shifted substantially from 8 mV in the single component system to -13 mV in the mixture system, indicating the attachment of weakly positively charged nano size alumina particles on to the highly negatively charged gas bubble surfaces. The second zeta potential distribution peak at -50 mV indicates the presence of

clean gas bubbles in the mixture system, possibly as a result of insufficient number of alumina particles present in the mixture system.

At pH 11, the bimodal zeta potential distribution of the mixture with the peak positions coinciding to the zeta potential distribution peak positions of the individual components suggests the absence of attractive forces between the two components. Considering strongly negatively charged nature for both alumina and gas bubbles at this pH, the observed absence of attachment is not unexpected due to strong electrical double layer forces.

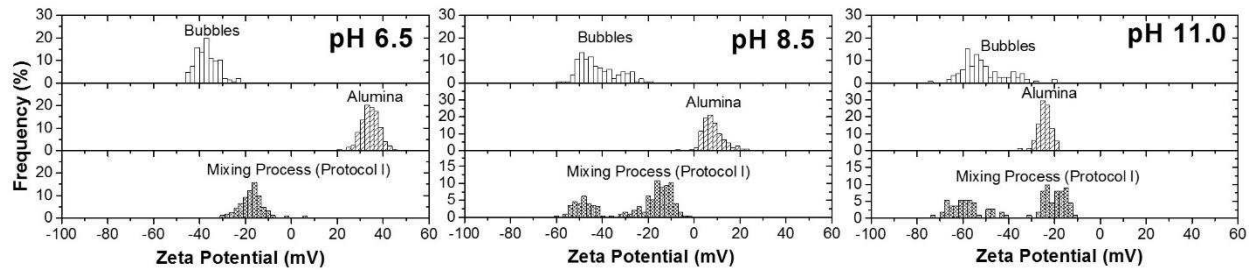


Figure 7. Zeta potential distribution of nano size alumina particles and bubbles prepared in 0.1 mM DF250 and 1 mM KCl solutions at pH 6.5, 8.5 and 11.0.

To support the experimental observations, the classical DLVO-type of interaction between an air bubble and alumina particle at pH 6.5, 8.5 and 11 in the presence of 0.1 mM DF250 were considered. In this study, the electrostatic double layer forces were calculated using the constant potential boundary conditions of air bubble and alumina particle: [2, 3]

$$V_T = V_A + V_R \quad [1]$$

$$V_R = -\frac{\pi\epsilon_0\epsilon a_1 a_2}{(a_1 + a_2)} \left( 2\Psi_1 \Psi_2 \ln \left[ \frac{1 + \exp(-\kappa H)}{1 - \exp(-\kappa H)} \right] + (\Psi_1^2 + \Psi_2^2) \ln[1 - \exp(-2\kappa H)] \right) \quad [2]$$

$$V_A = -\frac{A_{123}}{6H} \frac{a_1 a_2}{(a_1 + a_2)} \quad [3]$$

where  $V_T, V_A, V_R$  are the total, van der Waals attractive and electrical double layer contributes, respectively.  $a$  is the particle radius,  $\epsilon_0$  is the permittivity of vacuum,  $\epsilon$  is the relative dielectric

constant,  $\Psi$  is the surface potential,  $\kappa$  is the inverse Debye length,  $H$  is the separation distance and  $A$  is the Hamaker constant. Subscripts 1, 2 and 3 represent the air bubble, water and alumina particle, respectively. The calculated total interaction potential between the two components is shown in Fig. 8. At pH 6.5, the opposing surface potentials of the two components are sufficient to promote attraction in the secondary minimum at short separation distances. As pH increases, the attraction diminishes leading to a purely repulsive interaction at pH 11.0. The interaction energies as calculated using the classical DLVO are in good agreement with the attachment characteristics observed by zeta potential distribution analysis.

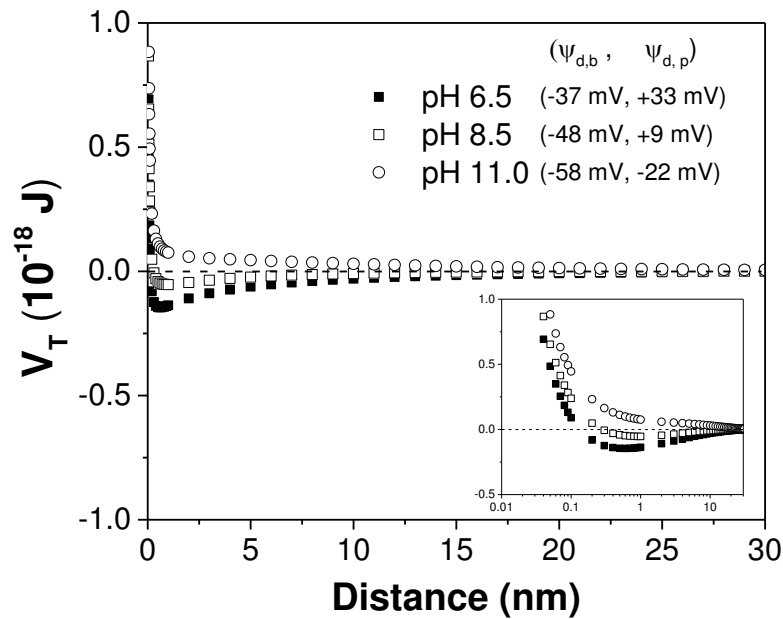


Figure 8. Total interaction energy between an air bubble and alumina particle as a function of solution pH, calculated using the classical DLVO theory (Eqs. 1-3). Inset: x-axis is plotted on a log scale to clearly highlight differences in the secondary minima at short separation distance. Experimental conditions:  $A_{123} = -3.750 \times 10^{-20}$  J,  $d_{air} = 350$  nm,  $d_{alumina} = 15$  nm, electrolyte = 1 mM KCl.

Preferential interactions in a tertiary system: The study was extended to assess the competitive interaction among the dispersed components in a tertiary (micron silica particles – micron alumina particles – gas bubbles) system. After preparation of dispersions using Protocol I in 0.1 mM DF250 + 1 mM KCl solutions of pH 6.5, the attachment characteristics between any two

components and among three components were determined. The results show contrasting zeta potential distributions between gas bubbles (peaked at -21 mV) and alumina particles (peaked at 51 mV), and a partial overlap of zeta potential distributions between the gas bubbles and silica particles (peaked at -44 mV). The binary systems of gas bubbles–alumina particles and gas bubbles–silica particles were then analyzed. With opposite signs of zeta potentials between gas bubbles and alumina particles, strong attachment between the two components was confirmed as shown by a single modal zeta potential distribution with the peak positioned at -17 mV, a value close to the zeta potential distribution peak value of single gas bubbles. This finding indicates a stable attachment of nano size bubbles on micron size alumina particles. In contrast, a clear bimodal zeta potential distribution was observed for the binary mixture of micron size silica and nano size bubbles with the distribution peaks located at approximately the same locations of corresponding individual components, indicating the repulsive forces between the two components. The strong repulsive forces are anticipated as both components are highly negatively charged.

To interpret the results of silica-alumina-bubble tertiary systems, it is important to determine the interactions between micron size alumina and silica particles. Since silica and alumina carry opposite surface charges, an attractive force between silica and alumina particles in their mixture is anticipated. However, the zeta potential distribution of silica-alumina mixture showed two peaks located at similar positions to the zeta potential distribution peaks of the individual components. The slight reduction in the alumina zeta potential distribution values and the small distribution centered at -20 mV indicates a very weak interaction between the two particles in the secondary minimum. This finding indicates the absence of strong attraction between the two particles, which is contradictory to the predictions from the classical DLVO theory. Considering the dynamic nature of the system under the agitation, it is possible that the disruptive force from hydrodynamic shear in the current system is sufficiently strong to tear apart the aggregates, leading to a dynamically dispersed system. [49] Also, interacting two particles of similar size is geometrically unfavorable for one particle to be completely coated by the second particle. Such behavior is in contrast to gas bubble – alumina interaction which confirmed the strong interaction between the two components with gas bubbles coating alumina particles. Smaller gas bubbles

and the ability to increase the contact area (spreading of the gas bubble on the alumina particle) create a condition that is stable to the hydrodynamic disruptive shear force.

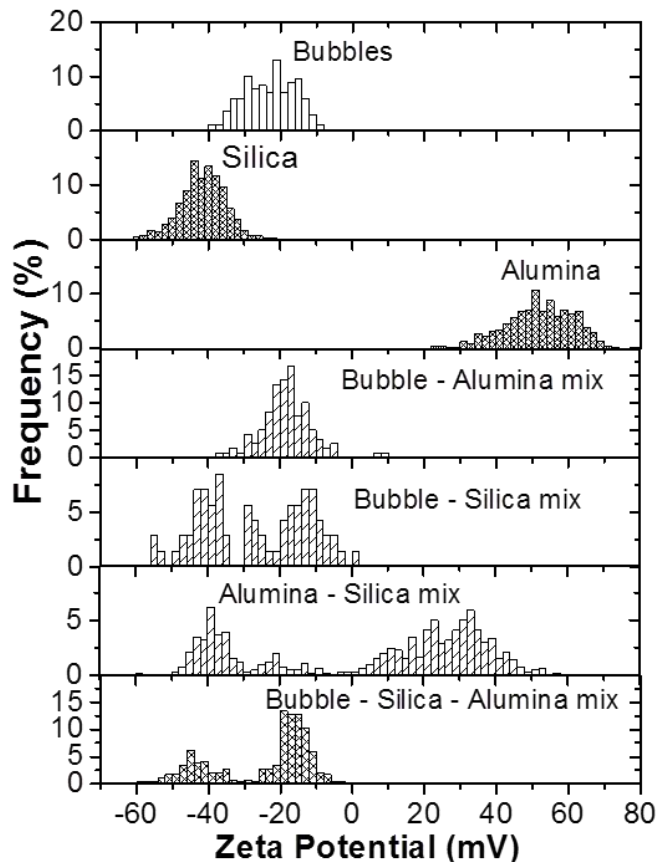


Figure 9. Zeta potential distribution analysis for primary, binary and tertiary systems. All dispersions prepared in 0.1 mM DF250 + 1 mM KCl solution at pH 6.5.

With the clear baseline results of binary systems, it is anticipated that bubbles will selectively attach to micron size alumina particles, leaving the silica particles dispersed. The results of zeta potential distribution measurement using silica–alumina–bubble tertiary mixture in Fig. 9 show a bimodal distribution, with distribution peaks being located at zeta potential values corresponding to the peaks of micron size silica particles (-45 mV) and mixture of alumina–bubble binary system (-17 mV). The loss of the alumina particle zeta potential distribution confirms the successful attachment of alumina particles and bubbles. The results confirm the hypothesis derived from the study of relevant binary systems and clearly demonstrate the feasibility of zeta

potential distribution measurement to study preferential interactions in a complex multicomponent (tertiary) system. However, it is clear that the zeta potential distribution technique is not applicable to the systems in which the individual components do not have their own distinct zeta potential distributions. For such systems, the quartz crystal microbalance (QCM) could be a good complementary technique,[50] provided that one of the components could be made as the surface of quartz crystal sensor.

## **Conclusions**

The need for greater characterization of the preferential interactions between particles in dynamic systems has led to the development of a new characterization method by zeta potential distribution analysis. The technique correlates the zeta potential distributions of individual components and the corresponding mixed component system to determine the degree and type of attachment. A range of systems have been studied to demonstrate the sensitivity of the technique when studying complex systems.

Comparing two methods of mixing, the present study has highlighted the importance of the mixing protocols in determining the strength of particle-gas bubble interactions. Such study helps realize the dual-bubble flotation principle where the target particle is first ‘frosted’ by smaller size nano bubbles prior to attachment to larger flotation bubbles. The preferential interaction between dispersed particles has been demonstrated for a complex tertiary particle system. While sub-micron gas bubbles are observed to favorably interact with micron size alumina particles, the interaction between micron size alumina and silica particles is limited by the aggregate instability in the flow.

The study demonstrates a new analysis method to determine the dominant interactions between several particle types in dynamic environments. The approach enables better understanding of the overall interactions that govern the collective behavior of the system.

## References

- [1] J.N. Israelachvili, *Intermolecular and Surface Forces*, Academic Press, 1991.
- [2] R. Hogg, T.W. Healy, D.W. Fuerstenau, *Trans Faraday Soc.* 62 (1966) 1638.  
doi:10.1039/TF9666201638.
- [3] K.J. Mysels, M.N. Jones, *Discuss Faraday Soc.* 42 (1966) 42. doi:10.1039/DF9664200042.
- [4] R.M. Pashley, *J Colloid Interface Sci.* 83 (1981) 531. doi:10.1016/0021-9797(81)90348-9.
- [5] L. Meagher, *J Colloid Interface Sci.* 152 (1992) 293. doi:10.1016/0021-9797(92)90030-P.
- [6] W.A. Ducker, T.J. Senden, R.M. Pashley, *Nature.* 353 (1991) 239. doi:10.1038/353239a0.
- [7] W.A. Ducker, Z. Xu, D.R. Clarke, J.N. Israelachvili, *J Am Ceram Soc.* 77 (1994) 437.  
doi:10.1111/j.1151-2916.1994.tb07012.x.
- [8] S. Nishimura, M. Kodama, H. Noma, K. Inoue, H. Tateyama, *Colloids Surf Physicochem Eng Aspects.* 143 (1998) 1. doi:10.1016/S0927-7757(98)00386-0.
- [9] R.M. Pashley, P.M. McGuiggan, B.W. Ninham, D.F. Evans, *Science.* 229 (1985) 1088.  
doi:10.1126/science.4035349.
- [10] P.M. Claesson, C.E. Blom, P.C. Herder, B.W. Ninham, *J Colloid Interface Sci.* 114 (1986) 234. doi:10.1016/0021-9797(86)90257-2.
- [11] D.Y.C. Chan, R.G. Horn, *J Chem Phys.* 83 (1985) 5311. doi:10.1063/1.449693.
- [12] S. Biggs, *Langmuir.* 11 (1995) 156. doi:10.1021/la00001a028.
- [13] H. Butt, M. Kappl, H. Mueller, R. Raiteri, W. Meyer, J. R uhe, *Langmuir.* 15 (1999) 2559.  
doi:10.1021/la981503+.
- [14] M.A. Hampton, A.V. Nguyen, *Adv Colloid Interface Sci.* 154 (2010) 30.  
doi:10.1016/j.cis.2010.01.006.
- [15] J.Y. Walz, A. Sharma, *J Colloid Interface Sci.* 168 (1994) 485.  
doi:<http://dx.doi.org/10.1006/jcis.1994.1446>.
- [16] D. Leckband, J. Israelachvili, *Q Rev Biophys.* 34 (2001) 105.  
doi:10.1017/S0033583501003687.
- [17] R. Yoon, L. Mao, *J Colloid Interface Sci.* 181 (1996) 613. doi:10.1006/jcis.1996.0419.

- [18] V.B. Menon, D.T. Wasan, *Colloids and Surfaces*. 19 (1986) 89. doi:DOI: 10.1016/0166-6622(86)80039-7.
- [19] T.H. Muster, C.A. Prestidge, R.A. Hayes, *Colloids Surf Physicochem Eng Aspects*. 176 (2001) 253. doi:DOI: 10.1016/S0927-7757(00)00600-2.
- [20] Z. Yan, J.A.W. Elliott, J.H. Masliyah, *J Colloid Interface Sci*. 220 (1999) 329. doi:DOI: 10.1006/jcis.1999.6533.
- [21] A. Yeung, T. Dabros, J. Masliyah, J. Czarnecki, *Colloids Surf Physicochem Eng Aspects*. 174 (2000) 169. doi:DOI: 10.1016/S0927-7757(00)00509-4.
- [22] Y. Xu, J. Wu, T. Dabros, H. Hamza, S. Wang, M. Bidal, J. Venter, T. Tran, *Can J Chem Eng*. 82 (2004) 829. doi:10.1002/cjce.5450820423.
- [23] Y. Xu, T. Dabros, H. Hamza, W. Shefantook, *Pet Sci Technol*. 17 (1999) 1051. doi:10.1080/10916469908949765.
- [24] L. Wang, D. Sharp, J. Masliyah, Z. Xu, *Langmuir*. 29 (2013) 3594. doi:10.1021/la304490e.
- [25] L. Wang, Z. Xu, J.H. Masliyah, *J Phys Chem C*. 117 (2013) 8799. doi:10.1021/jp4000945.
- [26] J. Liu, Z. Xu, J.H. Masliyah, *AIChE J*. 50 (2004) 1917.
- [27] J. Liu, J. Vandenberghe, J. Masliyah, Z. Xu, J. Yordan, *Minerals Eng*. 20 (2007) 566. doi:10.1016/j.mineng.2006.11.005.
- [28] M. Deng, Q. Liu, Z. Xu, *Minerals Eng*. 49 (2013) 165. doi:<http://dx.doi.org/10.1016/j.mineng.2013.05.014>.
- [29] M. Deng, Q. Liu, Z. Xu, *Minerals Eng*. 46-47 (2013) 6. doi:<http://dx.doi.org/10.1016/j.mineng.2013.03.013>.
- [30] F. Lin, L. Nolan, Z. Xu, K. Cadien, *J Electrochem Soc*. 159 (2012) H482. doi:10.1149/2.038206jes.
- [31] J. Liu, Z. Zhou, Z. Xu, J. Masliyah, *J Colloid Interface Sci*. 252 (2002) 409.
- [32] J. Liu, Z. Xu, J. Masliyah, *Langmuir*. 19 (2003) 3911.
- [33] H. Zhao, J. Long, J.H. Masliyah, Z. Xu, *Ind Eng Chem Res*. 45 (2006) 7482. doi:10.1021/ie060348o.
- [34] J. Liu, Z. Xu, J. Masliyah, *Can J Chem Eng*. 82 (2004) 655. doi:10.1002/cjce.5450820404.

- [35] J. Liu, Z. Xu, J. Masliyah, *J Colloid Interface Sci.* 287 (2005) 507.  
doi:10.1016/j.jcis.2005.02.037.
- [36] X. Ding, C. Repka, Z. Xu, J. Masliyah, *Can J Chem Eng.* 84 (2006) 643.  
doi:10.1002/cjce.5450840602.
- [37] E. Forbes, K.J. Davey, L. Smith, *Minerals Eng.* 56 (2014) 136.  
doi:<http://dx.doi.org/10.1016/j.mineng.2013.11.012>.
- [38] C. Wu, K. Nasset, J. Masliyah, Z. Xu, *Adv Colloid Interface Sci.* 179-182 (2012) 123.  
doi:10.1016/j.cis.2012.06.012.
- [39] D. Tao, S. Yu, X. Zhou, R.Q. Honaker, B.K. Parekh, *International Journal of Coal Preparation & Utilization.* 28 (2008) 1. doi:10.1080/07349340701640901.
- [40] Xu, Z., Choung, J., Sun, W., Z. Cui, (2006) 607 "Role of hydrodynamic cavitation by high intensity agitation in fine particle aggregation and flotation", in *Proceedings XXIII International Mineral Processing Congress*, Promedadvertising Agency, Istanbul, Turkey, 395-400.
- [41] M. Kosmulski, *J Colloid Interface Sci.* 275 (2004) 214.  
doi:<http://dx.doi.org/10.1016/j.jcis.2004.02.029>.
- [42] L. Huang, C. Maltesh, P. Somasundaran, *J Colloid Interface Sci.* 177 (1996) 222.  
doi:<http://dx.doi.org/10.1006/jcis.1996.0024>.
- [43] A.K. Vanjara, S.G. Dixit, *Langmuir.* 11 (1995) 2504. doi:10.1021/la00007a032.
- [44] Z.A. Zhou, Z. Xu, J.A. Finch, *Ind Eng Chem Res.* 37 (1998) 1998. doi:10.1021/ie970489d.
- [45] Z.A. Zhou, X. Zhenghe, J.A. Finch, *Minerals Eng.* 7 (1994) 1073.  
doi:10.1016/j.mineng.2008.12.010.
- [46] R.J. Atkinson, *J Colloid Interface Sci.* 42 (1973) 624. doi:[http://dx.doi.org/10.1016/0021-9797\(73\)90048-9](http://dx.doi.org/10.1016/0021-9797(73)90048-9).
- [47] L. Jiang, M. Krasowska, D. Fornasiero, P. Koh, J. Ralston, *Phys Chem Chem Phys.* 12 (2010) 14527. doi:10.1039/C0CP01367F.
- [48] B.V. Derjaguin, S.S. Dukhin, N.N. Rulyov, in, E. Matijević, R. Good (Eds.), *Springer US*, 1984, p. 71.
- [49] D. Harbottle, S. Biggs, M. Fairweather, *AIChE J.* 57 (2011) 1693. doi:10.1002/aic.12388.
- [50] M. Tamiz Bakhtiari, D. Harbottle, M. Curran, S. Ng, J. Spence, R. Siy, Q. Liu, J.H. Masliyah, Z. Xu, *Energy Fuels.* (2014). doi:10.1021/ef502088z.

